Journal of Experimental Botany, Vol. 71, No. 19 pp. 6074–6083, 2020
doi:10.1093/jxb/eraa306 Advance Access Publication 30 June 2020

RESEARCH PAPER

Canditate metabolites for ash dieback tolerance in *Fraxinus excelsior*

Miguel Nemesio-Gorriz[1,*], Riya C. Menezes[2], Christian Paetz[2], Almuth Hammerbacher[2,3], Marijke Steenackers[4], Kurt Schamp[4], Monica Höfte[5], Aleš Svatoš[2], Jonathan Gershenzon[2] and Gerry C. Douglas[1]

[1] Forestry Development Department, Teagasc, Dublin, Ireland
[2] Max Planck Institute for Chemical Ecology, Jena, Germany
[3] Department of Zoology and Entomology, Forestry and Agricultural Biotechnology Institute, University of Pretoria, Pretoria, South Africa
[4] Research Institute for Nature and Forest (INBO), Geraardsbergen, Belgium
[5] Department of Crop Protection, Faculty of Agricultural and Applied Biological Sciences, Ghent University, Ghent, Belgium

* Correspondence: miguel.nemesiogorriz@teagasc.ie

Received 14 January 2020; Editorial decision 15 June 2020; Accepted 23 June 2020

Editor: Howard Griffiths, University of Cambridge, UK

Abstract

Ash dieback, a forest epidemic caused by the invasive fungus *Hymenoscyphus fraxineus*, threatens ash trees throughout Europe. Within *Fraxinus excelsior* populations, a small proportion of genotypes show a low susceptibility to the pathogen. We compared the metabolomes from a cohort of low-susceptibility ash genotypes with a cohort of high-susceptibility ash genotypes. This revealed two significantly different chemotypes. A total of 64 candidate metabolites associated with reduced or increased susceptibility in the chemical families secoiridoids, coumarins, flavonoids, phenylethanoids, and lignans. Increased levels of two coumarins, fraxetin and esculetin, were strongly associated with reduced susceptibility to ash dieback. Both coumarins inhibited the growth of *H. fraxineus in vitro* when supplied at physiological concentrations, thereby validating their role as markers for low susceptibility to ash dieback. Similarly, fungal growth inhibition was observed when the methanolic bark extract of low-susceptibility ash genotypes was supplied. Our findings indicate the presence of constitutive chemical defense barriers against ash dieback in ash.

Keywords: Ash dieback, chemotype, coumarin, *Fraxinus*, *Hymenoscyphus*, secoiridoid, tolerance.

Introduction

In recent decades, European common ash (*Fraxinus excelsior*) has been severely affected by ash dieback (ADB) disease, caused by the invasive fungal pathogen *Hymenoscyphus fraxineus* (Baral *et al.*, 2014); it also infects narrow-leaved ash (*F. angustifolia*) (Kirisits *et al.*, 2010). *Hymenoscyphus fraxineus* was introduced in Europe and was first described in *F. excelsior* in Poland (Kowalski, 2006). Today, its distribution overlaps with most of the natural distribution of *F. excelsior*, with the exception of some areas in Southern and Western Europe. The pathogen infects the leaves of the host and translocates through the leaf rachis and petiole into the shoot, which leads to crown dieback. Over a number of years, this process results in crown loss and eventual death of ash trees (Gross *et al.*, 2014). Alternatively, conditions of high humidity and high infection pressure (Havrdová *et al.*, 2017) enable the pathogen to directly infect stem collars at ground level and

cause the trees to collapse from the base (Chandelier *et al.*, 2016; Enderle *et al.*, 2017), perhaps through the direct infection of stem lenticels (Nemesio-Gorriz *et al.*, 2019). The capacity of *H. fraxineus* to colonize living tissue in ash is the key to its success as a pathogen. High tree mortality rates are found in ash forests as a consequence of the action of the pathogen (Coker *et al.*, 2019). Despite the high susceptibility of *F. excelsior* to *H. fraxineus*, a small proportion of genotypes in ash populations show a low susceptibility to the pathogen. These genotypes appear as healthy trees with negligible disease symptoms in environments with high disease pressure and high tree mortality. It is not clear if host defense to ADB relies on induced or constitutive defense mechanisms. Genetic studies have shown that low susceptibility to ADB is genetically heritable (Muñoz *et al.*, 2016), polygenic in nature (Stocks *et al.*, 2019), and is stable in trees which are vegetatively propagated (Douglas *et al.*, 2017; Stener, 2018). After trees with low susceptibility are identified, they can be propagated with the aim of assembling collections as starting material for breeding populations (Plumb *et al.*, 2019) and for vegetative propagation (Douglas *et al.*, 2017). Low susceptibility to ADB is a polygenic trait that can be predicted using molecular markers (Stocks *et al.*, 2019). Once validated, markers for low susceptibility can aid greatly in the identification of ash genotypes and would facilitate selection among progeny from controlled and natural crosses.

Metabolomics profiling is an ideal tool to identify and understand factors for differentiating between different susceptibility groups (Cleary *et al.*, 2014; Sambles *et al.*, 2017; Sollars *et al.*, 2017), as it is a high-throughput technique and only requires small amounts of vegetative material. A metabolomics study in ash seedlings (Cleary *et al.*, 2014) identified metabolites associated with genotypic groups with different susceptibility after treatment with a fungal elicitor. Another study on *F. excelsior* leaf material identified five secoiridoids associated with high susceptibility to ADB in a Danish population of *F. excelsior* (Sambles *et al.*, 2017; Sollars *et al.*, 2017). A recent study differentiated genotypes with different susceptibility to ADB using advanced spectroscopy on bark samples (Villari *et al.*, 2018). Bark and leaf chemistry in ash show major quantitative and qualitative differences (Iossifova *et al.*, 1997). Even though leaves are the most common initial infection point for *H. fraxineus* (Gross *et al.*, 2014), the pathogen only causes substantial damage and dieback once it colonizes the phloem, making phloem a crucial tissue for defense. Even though previous studies have identified metabolites associated with groups of genotypes with different susceptibilities to ADB (Cleary *et al.*, 2014; Sambles *et al.*, 2017; Sollars *et al.*, 2017), specific candidate markers for reduced susceptibility to ADB were not validated by testing their activity on *H. fraxineus*. Therefore, the present study aimed to identify specific metabolites that are constitutively present in *F. excelsior* which associate with reduced susceptibility to ADB, and to validate their biological effects on the pathogen *in vitro*. The analyses included a large number of genotypes with a broad genetic background, from which bark samples were taken in the absence of the pathogen. The final objective was to identify and validate biochemical markers associated with low susceptibility to ADB. These markers may be useful as screening tools for plant material in breeding programs. This would save the significant amount of work, time, and resources associated with inoculation experiments and screenings for natural selection. At the same time, the study aimed to better understand the putative chemical defense mechanisms in *F. excelsior* against *H. fraxineus*.

To improve the clarity of the manuscript, definitions for the following terms are given: (i) resistance—situation of complete immunity to the pathogen in the host where the pathogen is unable to infect the host; (ii) tolerance—situation where the host allows infection to a small extent but this infection does not spread and the general health and growth rate of the host are not affected; (iii) susceptibility—failure by the host to contain the spread of the pathogen once it has been infected; susceptibility leads to major disease symptoms and, in some cases, to the death of the host; and (iv) defense—combination of physiological processes that allow the host to respond to the infection of a pathogen, resulting in resistance, tolerance, or susceptibility.

Materials and methods

Plant material

Sets of *F. excelsior* genotypes consisting of 19 low-susceptibility (LS) and 19 high-susceptibility (HS) genotypes to ADB were used for the metabolomics comparison. Scion wood from all the genotypes was grafted and grown under the same conditions in an unheated glasshouse in Dublin (Ireland). Current year shoots of all the genotypes, which had grown from the grafted plants, were used for the study. All shoots were healthy, with no evidence of dieback symptoms on leaves or stems. Details on the selection parameters of the HS and LS genotypes are given below.

High-susceptibility (HS) genotypes

Sixteen trees were selected in a 12-year-old European (RAP) provenance trial (https://cordis.europa.eu/project/rcn/58712/factsheet/en) of *F. excelsior* located in Slatta, Ireland. The trial consisted of 37 European provenances (three replicates per provenance each consisting of 36 trees) and border trees composed of one single lot of commercial Irish seedlings (common seed lot).

A further three trees were selected in a different provenance trial in the Manch Estate (Ireland). These trees belonged to two Irish provenances (Grantstown and Kilmacrennan) and one to the Danish seed orchard FP202 (https://static-curis.ku.dk/portal/files/21206956/final_wp34.pdf).

In the 3 years before this study, both trials above were monitored by the Irish Department of Agriculture for ADB symptoms and for the presence of *H. fraxineus* [quantitative PCR (qPCR) test; Chandelier *et al.*, 2010)] and found to be negative throughout the first 2 years. *Hymenoscyphus fraxineus* was confirmed in the third year of the trials when highly symptomatic plants were selected as the HS genotypes.

The 19 HS genotypes were selected amongst 5235 trees examined (3939 in Slatta and 1296 in Manch Estate). The HS trees were identified by cutting down a branch within the crown canopy and carefully assessing the stems for evidence of current year infection. Trees in which shoot dieback was present in >75% of the crown shoots were categorized as highly susceptible because of the quantity of shoots with symptoms which developed during the first year of infection by the pathogen. Details of the HS genotypes are given in Supplementary Table S1 at *JXB* online.

Low-susceptibility (LS) genotypes

Nineteen trees were selected as healthy trees in a 14-year-old European (RAP) provenance trial of *F. excelsior* (containing the same provenances as

the RAP trial in Ireland (see above; as well as 14 additional provenances from France). The trial is located in Stevoort, Belgium and established and monitored by the Research Institute for Nature and Forest (INBO).

In the year before this study (2012) started, the trial was monitored for ADB symptoms and the presence of *H. fraxineus* was confirmed. Subsequently, in the period 2013–2017, the symptoms of ADB were scored per tree annually. From 2013 to 2017, the percentage of dead trees as a result of ADB increased from 24.6% to 50.3%, confirming the high disease pressure in Stevoort. In 2017, the 19 LS trees were selected amongst 5508 examined.

The LS trees were selected as healthy trees on the basis of having <10% of shoot dieback in crowns and an absence of stem or collar infections. Details on the LS genotypes are given in Supplementary Table S1.

Sample preparation

Shoots from the current season of growth were cut in July from the grafted plants of each selected genotype; bark (including phloem) from internodes which were at least 5 cm long was stripped off, placed in 15 ml Falcon tubes, and immediately stored in liquid nitrogen until further use. Three samples per genotype were collected. Once in the laboratory, samples were homogenized using liquid nitrogen and porcelain mortars and pestles. Ground samples were freeze-dried and 50 mg of ground sample were used for extraction.

Each of the samples was extracted using 1500 µl of methanol (MeOH) shaking in a vortex for 30 min. Samples were then centrifuged for 15 min and 1000 µl of the supernatant was aspirated with a pipette. The supernatant was then run though a Macherey-Nagel Chromabond HR-X 1 ml/30 mg column to clean the sample.

Metabolomics analysis, candidate metabolite identification, and data analysis

HPLC-HRMS/MS measurements were recorded on a Bruker Compact O-TOF instrument controlled by Bruker O-TOF control ver.4.0 with chromatographic separation done on an Agilent Infinity 1260 HPLC. The HPLC measurements were conducted on a Agilent Zorbax SB-C18 column (3.5 µm, 4.6×150 mm), with a constant flow rate of 0.5 ml min^{-1} at 35 °C, a binary solvent system of H_2O+0.1% formic acid (A)/ MeCN+0.1% formic acid (B), and a linear gradient (%B): 0', 5%; 2', 5%; 10', 20%; 30', 40%; 36', 50%, 38', 95%; 47', 95%; 49', 5%; 50', 5%. The electron spray ionization (ESI) source parameters were as follows: negative polarity, a mass range of m/z 50–1300, end plate offset of 500 V, capillary voltage of 4500 V, nebulizer pressure at 1.8 bar, dry gas flow of 9.0 l min^{-1}, and a dry gas temperature of 220 °C. For small molecule MS/MS measurements with negative ionization, the standard settings provided by Bruker were used as follows: auto MS/MS, a mass range of m/z 20–40 000 with three precursors. The high-resolution LC-MS raw spectra were first centroided by converting them to mzXML format using the MS Convert feature of ProteoWizard 3.0.18324. Data processing was subsequently carried out with R Studio v1.1.463 using the Bioconductor XCMS package v 3.4.2 (Smith *et al.*, 2006; Tautenhahn *et al.*, 2008; Benton *et al.*, 2010), which contains algorithms for peak detection, peak deconvolution, peak alignment, and gap filling. The resulting peak list was uploaded into Metaboanalyst 4.0 (Chong *et al.*, 2018), a web-based tool for metabolomics data processing, statistical analysis, and functional interpretation where statistical analysis and modeling were performed. Missing values were replaced using a (K-nearest neighbor) KNN missing value estimation. Data filtering was implemented by detecting and removing non-informative variables that are characterized by near-constant values throughout the experimental conditions by comparing their robust estimate interquartile ranges (IQRs). Data were autoscaled. Out of the 3020 mass features originally detected, 2991 were used for the principal least square discriminant analysis (PLS-DA).

For the identification of candidate metabolites, the individual mass features that contributed to the separation between the different classes were further characterized by applying a range of univariate and multivariate statistical tests to determine their importance including the Pls-da importance variables, *t*-test, and random forest. The presence of each feature of interest was confirmed in the raw data and the molecular formula was estimated using Bruker Compass Data Analysis 5.1. This information, along with the retention time, accurate mass, and MS/MS spectra were used to probe into the existing literature and databases. MS/MS spectra files were also centroided and imported into GNPS (Wang *et al.*, 2016) for spectral matches and classical molecular networking. The dataset is available in the Dryad Digital Repository at doi:10.5061/dryad.7m0cfxpqv.

Bioassay on the effect of the methanolic extracts of LS and HS genotypes on the growth of H. fraxineus

The experiment was designed so that the methanolic extract from 15 g of fresh bark would be added to 15 ml of ash dust agar (ADA) medium to ensure that the fungus would grow in the presence of total metabolite concentrations equivalent to physiological bark concentrations. For the preparation of the extract, fresh shoots were collected from grafted plants of five HS genotypes (01B, 31A, 46D, 48C, and 56C) and five LS genotypes (37A, 39A, 39E, 45C, and 47A) from the same plants that were used for the metabolomics analysis. The selection of the genotypes was done based on material availability and a broad representation of the HS and LS groups in Fig. 1b. Current year shoots were harvested in July and brought into the lab, where an even mix of bark from each of the HS and LS genotypes was prepared by stripping off equal amounts of internodal sections manually; 15 g were weighed for each genotype group. The bark samples were then homogenized with liquid nitrogen using a porcelain mortar and a pestle. Ground samples were freeze-dried and then extracted by adding 20 ml of MeOH and shaking in a vortex for 30 min. The extract was then centrifuged for 15 min and the clear supernatant was decanted into a new 50 ml Falcon tube. The MeOH in the supernatant was then evaporated by applying nitrogen and, once evaporated, the extract was rediluted in 600 µl of MeOH.

Petri dishes (Ø 65mm) were filled with 5 ml of ADA (Botella *et al.*, 2016) each and were marked on the bottom with two perpendicular lines crossing their center, forming four axes that would aid colony growth measurement. Three Petri dishes were used for each treatment. The treatments were: control ADA, ADA supplemented with 200 µl (4%) of MeOH, ADA supplemented with 200 µl of the methanolic extract of HS genotypes, and ADA supplemented with 200 µl of the methanolic extract of LS genotypes. In each case, MeOH and methanolic extracts were dispensed carefully in small drops around the edge of the Petri dish. Once prepared, Petri dishes were allowed to dry for 30 min to let the MeOH evaporate. Petiole sections of 5 mm were co-cultured and colonized by the *H. fraxineus* isolate Erk2D (Bengtsson *et al.*, 2012), which was obtained from Dr Malin Elfstrand (Swedish University of Agricultural Sciences, Sweden). Colonized petiole sections were placed in the center of the dishes at the point where the two drawn lines intersected. Petri dishes were kept at room temperature in darkness over a period of 15 d, and a mark was made at the edge of the colonies on each of the four axes of the drawn lines. For each Petri dish, the mean value for each of the four axes was annotated, then the colony area was estimated using the formula $\pi \times r^2$. Colony area data were exported to Minitab17 (www.minitab.com), and ANOVA tests were performed to compare the mean colony area for each of the treatments and isolates.

Fungistatic effect of coumarins on H. fraxineus

Physiological concentrations of fraxetin and esculetin in extracts from LS and HS *F. excelsior* genotypes were estimated. For the estimation, the molar concentration of the coumarins was calculated based on the integral ratio between the sample (100 µl of bark extract from HS and LS genotypes) and the reference (1.30 mg of *p*-coumaric acid in 100 µl of MeOH). The molar concentration was multiplied by the molar masses of fraxetin (208.169 g mol^{-1}) and esculetin (178.14 g mol^{-1}). The amount of esculetin was in the range of 39.6–67.0 µg in HS samples and 92.4–211.9 µg in LS samples. The amount of fraxetin was in the range of 43.0–73.0 µg in HS samples and 100.6–230.6 µg in LS samples. The average amounts of coumarins in the bark extracts were used to estimate the physiological concentration in fresh bark considering that 50 mg of dry

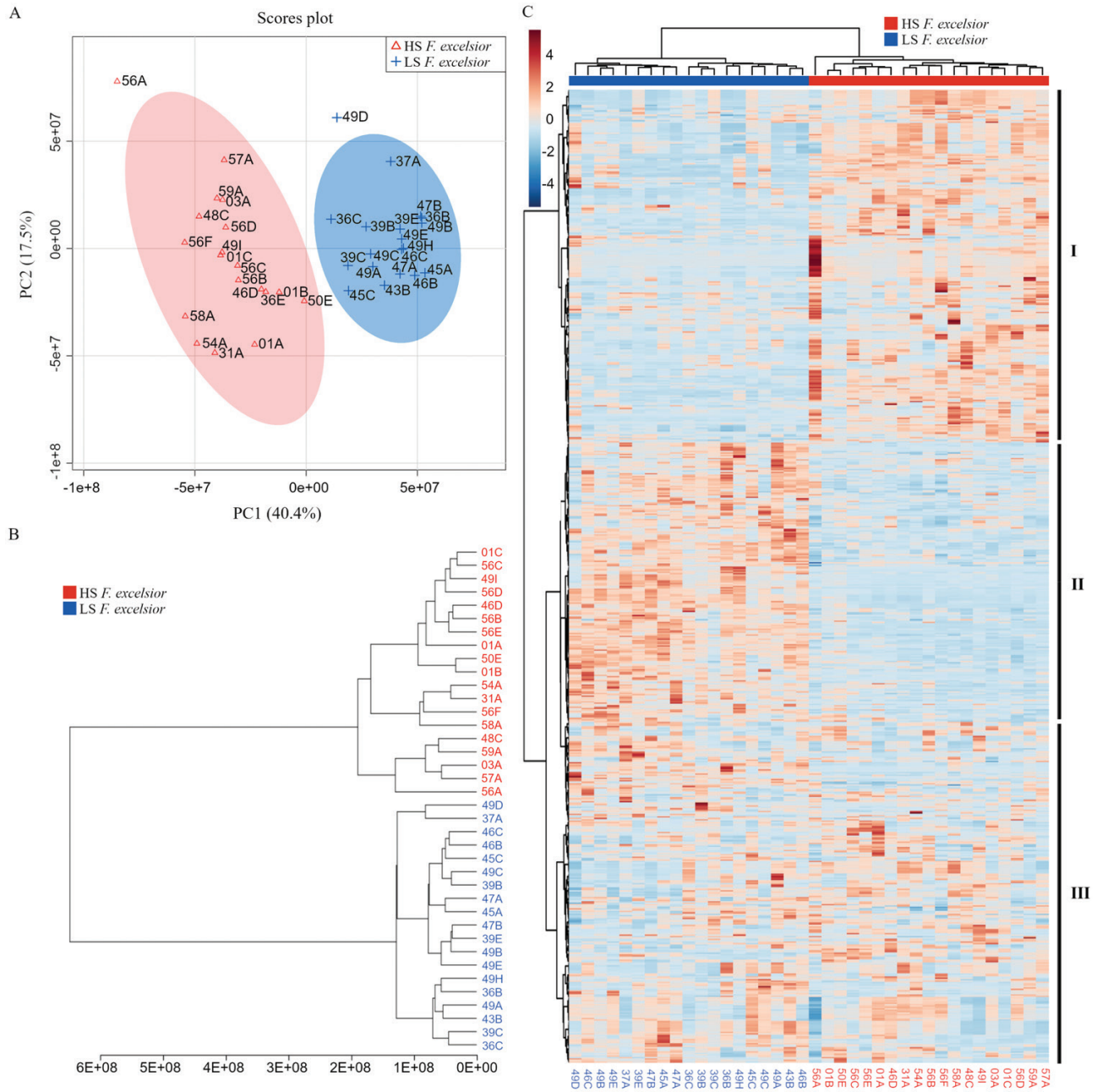

Fig. 1. Overview of the metabolomics comparison in methanolic bark extracts from *F. excelsior* genotypes with different susceptibilities to ash dieback. Two sets of samples were used, *F. excelsior* low susceptibility group (LS) (n=19), marked in blue, and *F. excelsior* high susceptibility group of (HS) (n=19), marked in red. (a) Representation of the results of the PCA analysis; (b) dendrogram representation of the comparison of the two groups (LS and S); (c) heatmap representing the relative abundance (log2) of 2982 mass features in each of the samples.

bark were extracted with 1500 µl of MeOH and that the average water content of fresh ash bark is 42%:

$$\frac{\text{Coumarin } \mu\text{g in } 100\ \mu\text{L}}{100\ \mu\text{L}} * \frac{1500}{50\,\text{mg}} * \frac{1000\,\text{mg}}{1\,\text{g}} * \frac{1\,\text{g fresh bark}}{(1-0.42)\,\text{g dry bark}} = \text{Coumarin } \mu\text{g per g of fresh bark}$$

The estimated physiological bark concentrations for esculetin were 53.3 µg g^{-1} and 152.2 µg g^{-1} for HS and LS genotypes, respectively. The estimated physiological bark concentrations for fraxetin were 58 µg g^{-1} and 165.6 µg g^{-1} for HS and LS genotypes, respectively. Three isolates of *H. fraxineus* (Erk2D, Ö3, and 21C) (Bengtsson *et al.*, 2012) were obtained from Dr Malin Elfstrand (Swedish University of Agricultural Sciences, Sweden) and subcultured in ADA (Botella *et al.*, 2016). Aliquots of 12 ml of ADA were measured in a 15 ml Falcon tube, where ADA was supplemented with 100 µl of DMSO (ADA control) or the corresponding LS and HS physiological concentrations of fraxetin (Sigma-Aldrich, 18224-50MG) and esculetin (Sigma-Aldrich, 246573-1G), which were pre-diluted in 100 µl of DMSO. The final DMSO concentration in all media was kept at 0.0083% in order to avoid toxicity to the isolates. Falcon tubes were inverted gently several times to mix the contents and were then poured into Ø 65 mm Petri dishes, which had been previously marked in the bottom with two perpendicular lines crossing their center, forming four axes that would aid colony growth measurement. In each case, a 5 mm petiole piece colonized by the corresponding *H. fraxineus* isolate (see method above) was placed in the center of each of the Petri dishes at the point where the two drawn lines intersected. Three technical replicates per treatment and per isolate were made. Petri dishes were kept at room temperature in darkness over a period of 15 d and a mark was

drawn at the edge of the colonies on each of the four axes of the drawn lines. For each Petri dish, the mean value for each of the four axes was annotated, then the colony area was estimated using the formula $\pi \times r^2$. Colony area data were exported to Minitab17 (www.minitab.com), and ANOVA tests were performed to compare the mean colony area for each of the treatments and isolates.

Results

HS and LS F. excelsior *genotypes represent two different* F. excelsior *chemotypes*

Statistical analysis of the metabolite profiles revealed two separate groups for *F. excelsior* corresponding to genotypes with a low susceptibility (LS) and those with a high susceptibility (HS) to ADB (Fig. 1). The PLS-DA revealed that PC1 accounted for 40.4% and PC2 accounted for 17.5% of the variance and contributed to the best separation of the groups. A 2D score plot was constructed and 95% confidence regions for each group marked, allowing clear discrimination of HS and LS genotypes based on their metabolic profiles. The two sample classes clustered separately and the HS group showed a higher variance (Fig. 1a). Furthermore, a dendrogram of the metabolic profiles of the analyzed genotypes showed two clearly separated subclusters corresponding to their level of susceptibility and not to their geographic origin, which is represented by the two first digits in each sample name (Fig. 1b). A heatmap representation of the relative levels for 2991 mass features for all the samples further supported a clear difference between HS and LS genotypes (Fig. 1c). Sections I and II of the map include mass features that are generally more abundant in either the HS or LS groups, respectively, while section III includes mass features with no association with either of the two groups.

Candidate metabolites associated with HS or LS to H. fraxineus

Out of 2991 mass features which were selected after filtering and quality control, a total of 64 candidate metabolites were identified as being associated with either HS or LS genotypes as a result of multiple statistical tests. Twenty-five of the candidates were more abundant in HS genotypes and 39 were more abundant in LS genotypes. For 53 of the candidates, a compound identity was annotated with confidence based on their accurate mass, MS/MS fragmentation matched with databases, and UV spectra, while 11 candidates were not identified. MS/MS fragmentation patterns of these candidates can be found in Supplementary Fig. S1. Based on their chemical family, 21 secoiridoids, eight coumarins, six lignans, six phenylethanoids, five flavonoids, four cinnamic acid esters, two monolignols, one shikimate derivative, and citric acid were positively identified (Table 1). From these, nine metabolites had been reported previously as important chemical defenses in ash (Cleary *et al.*, 2014; Sambles *et al.*, 2017; Sollars *et al.*, 2017). For each chemical family, details of the levels of the annotated metabolites in the HS and LS groups are presented in Supplementary Fig. S2. In addition, a detailed heatmap representing the levels of the 64 candidate metabolites in all the genotypes in the study can be found in Supplementary Fig. S3.

Fungistatic activity of the methanolic extract from bark samples taken from HS and LS genotypes

Our results show that, in terms of fungal growth, the largest colony area after 15 d was observed on control ADA medium (Fig. 2). The addition of 4% MeOH, even after letting it air-dry for 30 min, had a penalty on the growth of *H. fraxineus.* The addition of the methanolic extract from HS genotypes (in 4% MeOH) resulted in a similar colony area to the addition of 4% MeOH alone. The addition of the methanolic extract from LS genotypes (in 4% MeOH) completely inhibited the growth of *H. fraxineus* after 15 d, even though the fungus remained alive at the top of the inoculation plugs (Supplementary Fig. S4). A brownish coloration appeared in the medium for the Petri dishes that were supplemented with a bark methanolic extract. Supplementary Fig. S4 shows the Petri dishes at the end of the experiment (15 dpi).

Fungistatic activity of physiological concentrations of fraxetin and esculetin on H. fraxineus

Among the 39 candidate metabolites that were identified associated with LS genotypes, the two coumarins fraxetin and esculetin ranked first and fifth in terms of coefficient score (Table 1). Due to the high relevance and commercial availability of these coumarins, they were selected for a bioassay to determine their effects at physiological concentrations on three isolates of *H. fraxineus*.

A significant reduction in the growth of three *H. fraxineus* isolates (Erk2D, 21c, and Ö3) was observed after supplementing ADA medium with either fraxetin or esculetin. After 15 d, the colony area for all three fungal isolates was significantly reduced by the addition of the coumarins to the medium, depending on concentration (Table 2). For all three isolates, coumarin concentrations corresponding to the level found in LS genotypes (EsLS and FrLS) significantly inhibited fungal growth. At the physiological concentration of fraxetin in HS genotypes (FrHS), fungal growth inhibition was significant for isolate Erk2D and nearly significant for the two fungal isolates 21c and Ö3 (Table 2). For isolates 21c and Ö3, esculetin showed a stronger fungistatic effect compared with fraxetin even though it showed a lower coefficient mean score in our results. Isolate 21c was the least affected by the addition of the coumarins. For isolates Erk2D and Ö3, addition of esculetin at the physiological concentration for LS genotypes (EsLS) significantly reduced the colony area compared with the physiological concentration for HS genotypes (EsHS). For fraxetin, this was only observed in isolate Erk2D. In all cases, the addition of coumarins to the medium caused the appearance of a brown coloration.

Table 1. List of 64 candidate metabolites from bark extracts associated with LS and HS phenotypes of *F. excelsior*

Compound identity	Biochemical class	$[M-H]^-$ *m/z*	RT (min)	Coefficient mean score	*P*-value from *t*-test	More abundant in group
Fraxetin	Coumarins	207.029	15.75	97.76	2.25E-16	LS
Excelside B	Secoiridoids	685.227	18.54	96.52	2.49E-15	LS
Unknown	–	277.142	42.29	93.86	1.69E-13	LS
Unknown C26H34O13 hexoside	–	553.187	25.31	88.84	5.53E-11	LS
Esculetin	Coumarins	177.018	14.47	88.14	1.07E-10	LS
Unknown	–	387.154	43.91	86.94	3.09E-10	LS
Unknown	Secoiridoids	1133.324	18.64	86.86	3.31E-10	LS
Calceolarioside B	Phenylethanoids	477.136	17.75	86.41	4.84E-10	LS
Unknown C21H10O9	–	405.029	4.27	86.13	6.13E-10	LS
Ligstroside-related	Secoiridoids	909.294	27.83	85.98	6.90E-10	LS
Syringaresinol beta-D-diglucoside-related	Lignans	787.260	15.14	83.65	4.09E-09	LS
Quinic acid-related	Shikimates	463.146	9.19	82.48	9.28E-09	LS
Isofraxidin	Coumarins	221.044	13.82	82.45	9.46E-09	LS
Angustifolioside A	Secoiridoids	701.222	18.02	81.24	2.11E-08	LS
Unknown hexoside	–	489.159	14.97	80.27	3.85E-08	LS
Fraxidin hexoside	Coumarins	383.097	14.47	78.26	1.26E-07	LS
Angustifolioside B	Secoiridoids	685.228	18.16	76.99	2.51E-07	LS
Oleoside methyl ester-related C23H36O16	Secoiridoids	567.189	12.20	74.93	7.19E-07	LS
Syringaresinol beta-D-glucoside	Lignans	579.202	19.09	72.65	2.10E-06	LS
Fraxiresinol hexoside	Lignans	565.188	17.01	70.15	6.17E-06	LS
Isokaempferide	Flavonoids	299.053	33.32	69.72	7.34E-06	LS
Oleoside	Secoiridoids	389.109	9.96	68.95	9.99E-06	LS
Pinoresinol diglucoside	Lignans	681.235	14.44	67.39	1.82E-05	LS
Unknown C17H28O11	–	407.155	10.64	66.81	2.26E-05	LS
Insularoside 3',6''-diglucoside	Secoiridoids	951.288	18.40	66.24	2.78E-05	LS
Ferulic acid	Cinnamic acid	193.049	23.05	63.70	6.70E-05	LS
Kaempferol-3-*O*-glucoside	Flavanoids	447.089	19.32	62.52	9.87E-05	LS
Oleuropein	Secoiridoids	539.171	19.79	54.30	0.0010	LS
Naringenin	Flavanoids	271.058	30.64	52.49	0.0016	LS
Calceolarioside A	Phenylethanoids	477.136	17.33	46.35	0.0061	LS
Isoligstroside	Secoiridoids	523.176	25.64	45.20	0.0076	LS
Ligstroside	Secoiridoids	523.177	24.76	44.17	0.0093	LS
10-HyhHHdroxyoleuropein	Secoiridoids	555.166	17.54	41.36	0.0155	LS
Unknown	–	943.335	30.43	38.17	0.0265	LS
Oleoside methylester-related	Secoiridoids	787.226	14.13	34.85	0.0440	LS
Oleoside-related	Secoiridoids	955.287	12.53	28.58	0.1017	LS
Nuzhenide	Secoiridoids	685.227	18.95	24.09	0.1702	LS
Fraxin-related	Coumarins	911.240	13.71	13.75	0.4376	LS
Hydroxytyrosol 1-*O*-glucoside	Phenylethanoids	315.108	9.77	12.81	0.4696	LS
Quercetin 3-*O*-rutinoside	Flavonoids	609.141	16.57	90.16	1.46E-11	HS
5-*O*-Caffeoylshikimate	Coumarins	335.075	15.05	88.08	1.12E-10	HS
4-Coumaroylshikimic acid	Monolignols	319.080	17.43	85.21	1.27E-09	HS
Formate adduct of tyrosol glucoside	Phenylethanoids	345.118	11.39	81.73	1.53E-08	HS
Citric acid	Small organic acid	191.020	3.14	79.63	5.69E-08	HS
Chlorogenic acid	Monolignols	353.087	10.88	71.43	3.59E-06	HS
Isoquercetin	Flavonoids	463.084	17.52	65.13	4.13E-05	HS
Verbascoside	Cinnamic acid esters	623.193	16.79	63.81	6.46E-05	HS
Esculin	Coumarins	339.071	11.99	60.72	0.0002	HS
Pinoresinol 4-*O*-beta-D-glucopyranoside	Lignans	519.181	18.78	59.96	0.0002	HS
7-beta-D-Glucopyranosyl-11-methyloleoside	Secoiridoids	565.174	13.32	59.50	0.0002	HS
Isoacteoside	Secoiridoids	623.193	17.20	55.35	0.0008	HS
Frameroside	Secoiridoids	601.208	24.11	54.97	0.0009	HS
Formate adduct of Phenylethyl primeveroside	Phenylethanoids	461.164	15.71	54.27	0.0010	HS
3-*O*-Feruloylquinic acid	Cinnamic acid esters	367.101	15.63	49.83	0.0029	HS
8-Hydroxypinoresinol 8-glucoside	Lignans	535.178	16.30	49.07	0.0034	HS
Formate adduct of unknown C18H26O11	–	463.141	17.93	48.22	0.0041	HS
Uhdenoside	Secoiridoids	525.158	16.42	44.71	0.0084	HS
Unknown	–	569.181	22.84	42.99	0.0116	HS

Table 1. Continued

Compound identity	Biochemical class	[M-H]⁻ *m/z*	RT (min)	Coefficient mean score	*P*-value from *t*-test	More abundant in group
Unknown	–	445.121	3.01	37.19	0.0309	HS
N2	Secoiridoids	565.174	12.60	26.55	0.1295	HS
Quinic acid-related	Cinnamic acid esters	353.086	12.94	24.33	0.1659	HS
Ligstroside-related	–	909.292	28.45	20.12	0.2538	HS
Oleoside-11-methyl ester	Secoiridoids	403.122	14.16	15.20	0.3904	HS
Fraxin	Coumarins	369.081	13.69	6.47	0.7155	HS

For each of the candidates, compound identification, biochemical class, molecular mass ([M-H]⁻ *m/z*), retention time in minutes (RT), and in which group (HS or LS) the metabolite is more abundant. The importance measure (coefficient mean score) represents on a scale from 0 to 100 the relative importance of each compound at separating the LS and HS groups and is based on a weighted sum of the PLS regression coefficients. The weights are a function of the reduction of the sums of squares across the number of principal least square components.

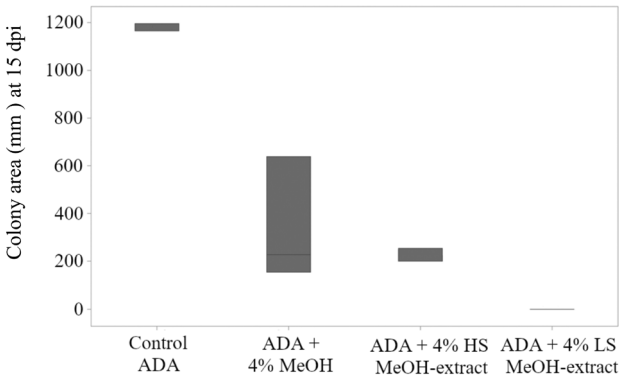

Fig. 2. Effects of methanolic extracts of bark from five HS and five LS *F. excelsior* genotypes on growth of *H. fraxineus*. Colony area after 15 d of growth of the *H. fraxineus* isolate Erk2D on control (ADA medium), ADA supplemented with 4% MeOH, ADA supplemented with 4% methanolic extract of five high-susceptibility (HS) ash genotypes, and ADA supplemented with 4% methanolic extract of five low-susceptibility (LS) ash genotypes (n=3).

Discussion

Plant metabolites are key components in the regulation of biotic interactions at cell level between pathogens and hosts. Our results indicate that LS and HS *F. excelsior* genotypes represent two different chemotypes in *F. excelsior*, with large differences in their metabolomics profiles, some of which were associated with the susceptibility to *H. fraxineus*. Biotic interactions are major factors driving natural selection (Wheat *et al.*, 2007). These interactions have been associated with the presence of different chemotypes in several plant species in response to the action of pests and pathogens (Christensen *et al.*, 2014; Calf *et al.*, 2019). Previous studies showed that susceptibility to ADB in *F. excelsior* is a quantitative trait (Lobo *et al.*, 2014; Muñoz *et al.*, 2016; Stocks *et al.*, 2019) that depends on multiple individual factors, each with a small effect. This study identified a total of 64 metabolites associated with increased and reduced susceptibility to *H. fraxineus* (Table 1). As can be appreciated in Fig. 1c and Supplementary Fig. S2, individual genotypes showing HS or LS might contain or lack only a portion of these factors, making signals difficult to identify and associate with a given phenotype. This difficulty can be present in experiments where population admixture occurs in the experimental set-up (Deng, 2001), leading to incorrect associations between signals and phenotype. Similar to Villari *et al.* (2018), a broad selection of ash genotypes from multiple provenances in several countries was used in this study to avoid confounding effects. Furthermore, HS and LS plants were grown as grafted plants from healthy scion wood in the same conditions, and samples for extractions were made in triplicate per genotype in order to minimize environmental error sources. Villari *et al.* (2018) could not observe an environmental footprint in bark chemistry in samples taken from six different European locations. Similarly, a study in *Quercus agrifolia* showed no differences in phenolics between healthy bark tissue and bark tissue sampled 60 cm away from canker caused by *Phytophtora ramorum* (Ockels *et al.* 2007). While there is enough evidence that the samples in this study could be considered free from footprints left by their previous contact with *H. fraxineus* or their original environment, this hypothesis cannot be completely discarded. As genome-wide genotyping tools for ash become available in the future (Sollars *et al.*, 2017; Stocks *et al.*, 2019), it will be possible to associate increased or reduced levels of specific metabolites with DNA variations, with the aim of understanding the genetic basis behind the biosynthesis of specific metabolites responsible for ash defense.

Genotype selection was further validated by the results of the bioassay, which show that the addition of the methanolic bark extract of HS to ADA medium resulted in a similar colony growth to the control, while the addition of the methanolic extract of LS genotypes to ADA resulted in a complete growth inhibition of *H. fraxineus* (Fig. 2). The results of this experiment showed that the factors causing fungal inhibition were found in the methanolic extract of *F. excelsior* bark. We observed that addition of bark extracts or of coumarins to the medium resulted in a brownish coloration in the medium with the fungus. Future studies may investigate how *H. fraxineus* detoxifies ash metabolites and increase the understanding of this plant–pathogen interaction. It is known that *H. fraxineus* in Europe has a very low genetic diversity (Burokiene *et al.*, 2015; McMullan *et al.*, 2018). In the present study, the results of the bioassay to test the individual effect of fraxetin and esculetin on fungal growth showed a variation in the tolerance to the different treatments in the different isolates (Table 2). This indicates that the pathogen has a certain capacity to adapt to some of the natural defense barriers in *F. excelsior*. As a consequence, new strains of *H. fraxineus* should be prevented from arriving in Europe in the future as a larger genetic diversity might

Table 2. Effect of physiological concentrations of esculetin and fraxetin on growth (mm^2) of three isolates of *H. fraxineus*

a	Area d15±SD	b	Control	EsHS	EsLS	FrHS	FrLS
21c		21c					
Control	1680±60	Control	1	0.009	0.007	0.053	0.009
EsHS	1532±53	EsHS		1	0.182	0.875	0.326
EsLS	1277±269	EsLS			1	0.191	0.321
FrHS	1545±122	FrHS				1	0.930
FrLS	1529±277	FrLS					1
Erk2D		Erk2D					
Control	1711±68	Control	1	0.000	0.000	0.010	0.000
EsHS	1452±34	EsHS		1	0.048	0.417	0.005
EsLS	1279±101	EsLS			1	0.052	0.127
FrHS	1510±106	FrHS				1	0.009
FrLS	1126±94	FrLS					1
Ö3		Ö3					
Control	1651±105	Control	1	0.007	0.000	0.062	0.006
EsHS	1224±249	EsHS		1	0.018	0.156	0.374
EsLS	625±91	EsLS			1	0.000	0.000
FrHS	1492±93	FrHS				1	0.133
FrLS	1292±159	FrLS					1

(a) Colony areas after 15 ds of growth for fungal isolates: 21c, Erk2D, and Ö3 on ADA medium (control) and ADA supplemented with physiological concentrations of esculetin (Es) and fraxetin (Fr), estimated in high susceptibilty (HS) and low susceptibilty (LS) groups: esculetin (EsHS; 53.3 μg ml^{-1} and EsLS, 152.2 μg ml^{-1}) and fraxetin (FrHS, 58 μg ml^{-1} and FrLS, 165.6 μg ml^{-1}). (b) *P*-value of the comparisons between different treatments. Significant differences are highlighted in grey.

allow *H. fraxineus* to adapt more efficiently to the natural defense barriers in *F. excelsior*.

A total of eight coumarins were found among our candidate metabolites, with six of them showing high coefficient scores. Among them, fraxetin and esculetin were tested against the fungus. Both coumarins showed a fungistatic effect on *H. fraxineus* at physiological concentrations, validating their role as biochemical markers for tolerance to *H. fraxineus* in *F. excelsior*. Coumarins are naturally abundant in *Fraxinus* species (Kostova and Iossifova, 2007), and at the same time their levels are highly variable (Whitehill *et al.*, 2012), making them ideal candidates for intra- and interspecific variation in pest resistance in ash. Interestingly, levels of the glycosylated forms of fraxetin and esculetin (fraxin and esculin, respectively) were less abundant in LS genotypes. Similarly, a study on emerald ash borer (EAB) resistance in ash found reduced levels of the glycoside esculin in EAB-resistant *F. mandshurica* compared with EAB-susceptible *F. nigra* (Villari *et al.*, 2016). A previous study showed that the glycosylated coumarins have a much lower antifungal activity compared with their respective aglycones (Mercer *et al.*, 2013). Our results may suggest that LS genotypes can retain a higher amount of coumarins in their non-glycosylated form, thus increasing the antimicrobial capacity of the coumarinic portion in LS genotypes. The importance of coumarins in ash defense might involve more organisms than just ADB. EAB is an invasive insect that has brought several ash species in North America to the brink of extinction (Herms and McCullough, 2014). Studies have found that those ash species susceptible to EAB show a lack of coumarins, with the exception of scopoletin, compared with EAB-resistant ash species (Whitehill *et al.*, 2012;Villari *et al.*, 2016; Qazi *et al.*, 2018). A recent study showed proof of convergent evolution in substrate recognition sites for an enzyme targeting *p*-coumarate, a coumarin precursor, in EAB-resistant ash species (Kelly *et al.* 2020). Phenylcoumaran benzylic ether reductase, an enzyme that targets coumarin precursors (Niculaes *et al.*, 2014), was identified in a proteomics study as a candidate enzyme linked to the resistance of *F. mandshurica* to EAB (Whitehill *et al.*, 2011). Studies in other plant species cover the biosynthesis of coumarins (Karamat *et al.*, 2014; Shimizu, 2014;Vanholme *et al.*, 2019) and its regulation (Chezem *et al.*, 2017), but the topic remains poorly understood. Because of the natural abundance and diversity of coumarins and their role in plant defense, Fraxinus species are ideal model species to study the mechanisms behind the biosynthesis and regulation of these compounds. As more genomic resources are made available (Sollars *et al.*, 2017), this objective should be achievable.

Candidate metabolites from other chemical families including secoiridoids, flavonoids, lignans, and phenylethanoids were identified in this study. This broad range of metabolites reflects the diversity in mechanisms on which *F. excelsior*'s defense against *H. fraxineus* relies. Among the candidate metabolites, 21 were secoiridoids. This large diversity of secoiridoids reflects the importance of this compound family in defense against *H. fraxineus* in *F. excelsior*. Two secoiridoids previously reported as N2 (Excelside A-like compound) and N4 (Nuzhenide) (Sambles *et al.*, 2017; Sollars *et al.*, 2017) were also identified in our study, but neither of them showed significant differences between the HS and LS groups. Two other secoiridoids associated with LS genotypes, oleuropein and 10-hydroxyoleuropein, were previously reported to associate with LS for *F. excelsior* seedlings after treatment with a *H. fraxineus* fungal elicitor (Cleary *et al.*, 2014). Collectively, secoiridoids have been associated with increased susceptibility to ADB in ash (Sambles *et al.*, 2017; Sollars *et al.*, 2017) and with reduced susceptibility to ADB (Cleary *et al.*, 2014) and to EAB (Villari *et al.*, 2016). In this study, 15 secoiridoid candidates were associated with LS genotypes and six were associated with HS genotypes. Secoiridoids vary in their antimicrobial and antioxidant properties, which depend on small changes in their structure (Božunović *et al.*, 2018). It is possible that a different transcriptional regulation in secoiridoid biosynthesis leads HS and LS genotypes to accumulate secoiridoids with different activity against *H. fraxineus*.

The present study showed that five flavonoids were identified and associated with different susceptibility to ADB. Two quercetin glycosides, rutin and isoquercetin, were associated with HS genotypes, while naringenin and kaempferide were associated with LS genotypes. Interestingly, rutin, which is associated with the HS group in our study, has been previously associated with increased fungal susceptibility in apple (Petkovsek *et al.*, 2007). Flavonoids play an important role in plant–microbe interactions (Hassan and Mathesius, 2012) including plant–microbe crosstalk and antimicrobial functions. This study indicates that flavonoids play a role in susceptibility to ADB. Six lignans were annotated in this study. Lignans have been reported previously in resistance to EAB in ash (Whitehill

et al., 2011, 2012; Villari *et al*., 2016; Qazi *et al*., 2018). Apart from their role in insect defense, lignans have antifungal properties (Cho *et al*., 2007), which could play a role in the interaction between ash and *H. fraxineus*. Lastly, six phenylethanoids were annotated in this study as candidate metabolites, two of which were present to a greater extent in HS genotypes while four were in HS genotypes, including calceolarioside A and B, which were previously associated with resistance against EAB in *F. mandshurica* (Eyles *et al*., 2007; Whitehill *et al*., 2012).

In conclusion, this study presents the most complete list of ash metabolites associated with reduced and increased susceptibility to ADB including metabolites identified in previous studies. Within each of the chemical families into which the candidate metabolites were classified, a portion of the candidates associated with either the HS or the LS genotypes. Our findings suggest that differences between the chemotypes associated with the HS and LS groups are unlikely to be caused by one or a few enzymes within biosynthetic pathways but rather by the action of transcriptional regulatory elements. The differences in the levels of metabolites between HS and LS ash groups were present in bark samples which had not been previously inoculated or treated with fungal elicitors, suggesting that at least a part of the defense mechanisms against *H. fraxineus* in ash are constitutive chemical barriers. Additionally, an important portion of the candidate metabolites in this study have been reportedly associated with resistance to EAB in ash, suggesting the possibility of parallel mechanisms conferring resistance against EAB and ADB simultaneously. The study presents new biochemical markers in ash and, for the first time, validates the fungistatic properties of fraxetin and esculetin on *H. fraxineus* and their role as markers for tolerance in ash.

Supplementary data

Supplementary data are available at *JXB* online.

Table S1. List of the genotypes used in this study.

Fig. S1. MS/MS fragmentation of the ions of the 64 relevant metabolites in negative ionization mode

Fig. S2. A boxplot representation for each of the 64 candidate metabolites of the relative levels in HS and LS genotypes.

Fig. S3. Heatmap representation of the levels of 64 candidate metabolites identified in this study.

Fig. S4. Fungistatic activity of the methanolic extracts from HS and LS genotypes of *F. excelsior* on the isolate Erk2D of *H. fraxineus*.

Acknowledgements

The authors acknowledge the financial support of the Irish Department of Agriculture Food and Marine for this FORM project and COST, which through the action FA1306 provided the funds for the study visit at the Max Planck Institute for Chemical Ecology, in which samples were analyzed. The authors acknowledge all the people and institutions who contributed to the establishment of the RAP trials, which allowed the selection of plant material in this study. The authors also thank the generosity of Dr Malin Elfstrand, who provided *H. fraxineus* isolates for the fungal bioassays, and the Gaelic Athletic Association (GAA) for facilitating exchanges of personnel during the study.

Data availablity

The dataset for this study has been deposited in the Dryad Data Repository at doi:10.5061/dryad.7m0cfxpqv (Nemesio-Gorriz *et al*., 2020).

References

Baral HO, Queloz V, Hosoya T. 2014. *Hymenoscyphus fraxineus*, the correct scientific name for the fungus causing ash dieback in Europe. IMA Fungus **5**, 79–80.

Bengtsson SB, Vasaitis R, Kirisits T, Solheim H, Stenlid J. 2012. Population structure of *Hymenoscyphus pseudoalbidus* and its genetic relationship to *Hymenoscyphus albidus*. Fungal Ecology **5**, 147–153.

Benton HP, Want EJ, Ebbels TM. 2010. Correction of mass calibration gaps in liquid chromatography–mass spectrometry metabolomics data. Bioinformatics **26**, 2488–2489.

Botella L, Čermáková V, Bačová A, Dvořák M. 2016. ADA, a fast-growth medium for *Hymenoscyphus fraxineus*. Forest Pathology **46**, 85–87.

Božunović J, Živković S, Gašić U, Glamočlija J, Ćirić A, Matekalo D, Šiler B, Soković M, Tešić Ž, Mišić D. 2018. In vitro and in vivo transformations of *Centaurium erythraea* secoiridoid glucosides alternate their antioxidant and antimicrobial capacity. Industrial Crops and Products **111**, 705–721.

Burokiene D, Prospero S, Jung E, Marciulyniene D, Moosbrugger K, Norkute G, Rigling D, Lygis V, Schoebel CN. 2015. Genetic population structure of the invasive ash dieback pathogen *Hymenoscyphus fraxineus* in its expanding range. Biological Invasions **17**, 2743–2756.

Calf OW, Huber H, Peters JL, Weinhold A, Poeschl Y, van Dam NM. 2019. Gastropods and insects prefer different *Solanum dulcamara* chemotypes. Journal of Chemical Ecology **45**, 146–161.

Chandelier A, André F, Laurent F. 2010. Detection of *Chalara fraxinea* in common ash (*Fraxinus excelsior*) using real time PCR. Forest Pathology **40**, 87–95.

Chandelier A, Gerarts F, San Martin G, Herman M, Delahaye L. 2016. Temporal evolution of collar lesions associated with ash dieback and the occurrence of *Armillaria* in Belgian forests. Forest Pathology **46**, 289–297.

Chezem WR, Memon A, Li FS, Weng JK, Clay NK. 2017. SG2-type R2R3-MYB transcription factor MYB15 controls defense-induced lignification and basal immunity in Arabidopsis. The Plant Cell **29**, 1907–1926.

Cho JY, Choi GJ, Son SW, Jang KS, Lim HK, Lee SO, Sung ND, Cho KY, Kim JC. 2007. Isolation and antifungal activity of lignans from *Myristica fragrans* against various plant pathogenic fungi. Pest Management Science **63**, 935–940.

Chong J, Soufan O, Li C, Caraus I, Li S, Bourque G, Wishart DS, Xia J. 2018. MetaboAnalyst 4.0: towards more transparent and integrative metabolomics analysis. Nucleic Acids Research **46**, W486–W494.

Christensen S, Heimes C, Agerbirk N, Kuzina V, Olsen CE, Hauser TP. 2014. Different geographical distributions of two chemotypes of *Barbarea vulgaris* that differ in resistance to insects and a pathogen. Journal of Chemical Ecology **40**, 491–501.

Cleary MR, Andersson PF, Broberg A, Elfstrand M, Daniel G, Stenlid J. 2014. Genotypes of *Fraxinus excelsior* with different susceptibility to the ash dieback pathogen *Hymenoscyphus pseudoalbidus* and their response to the phytotoxin viridiol—a metabolomic and microscopic study. Phytochemistry **102**, 115–125.

Coker TL, Rozsypálek J, Edwards A, Harwood TP, Butfoy L, Buggs RJ. 2019. Estimating mortality rates of European ash (*Fraxinus excelsior*) under the ash dieback (*Hymenoscyphus fraxineus*) epidemic. Plants, People, Planet **1**, 48–58.

Deng HW. 2001. Population admixture may appear to mask, change or reverse genetic effects of genes underlying complex traits. Genetics **159**, 1319–1323.

Douglas GC, McNamara J, O'Connell K, Dunne L, Grant J. 2017. Vegetative propagation of dieback-tolerant *Fraxinus excelsior* on a commercial scale. In: Vasaitis R, Enderle R eds. Dieback of European Ash (*Fraxinus* spp.): consequences and guidelines for sustainable management, the report on European Cooperation in Science & Technology (COST) Action FP1 103 FRAXBACK. Swedish University of Agricultural Sciences, 288–299.

Enderle R, Sander F, Metzler B. 2017. Temporal development of collar necroses and butt rot in association with ash dieback. iForest-Biogeosciences and Forestry **10**, 529–536.

Eyles A, Jones W, Riedl K, Cipollini D, Schwartz S, Chan K, Herms DA, Bonello P. 2007. Comparative phloem chemistry of Manchurian (*Fraxinus mandshurica*) and two North American ash species (*Fraxinus americana* and *Fraxinus pennsylvanica*). Journal of Chemical Ecology **33**, 1430–1448.

Gross A, Holdenrieder O, Pautasso M, Queloz V, Sieber TN. 2014. *Hymenoscyphus pseudoalbidus*, the causal agent of European ash dieback. Molecular Plant Pathology **15**, 5–21.

Hassan S, Mathesius U. 2012. The role of flavonoids in root–rhizosphere signalling: opportunities and challenges for improving plant–microbe interactions. Journal of Experimental Botany **63**, 3429–3444.

Havrdová L, Zahradník D, Romportl D, Pešková V, Černý K. 2017. Environmental and silvicultural characteristics influencing the extent of ash dieback in forest stands. Baltic Forestry **23**, 168–182.

Herms DA, McCullough DG. 2014. Emerald ash borer invasion of North America: history, biology, ecology, impacts, and management. Annual Review of Entomology **59**, 13–30.

Iossifova T, Kostova I, Evstatieva LN. 1997. Secoiridoids and hydroxycoumarins in Bulgarian *Fraxinus* species. Biochemical Systematics and Ecology **25**, 271–274.

Karamat F, Olry A, Munakata R, Koeduka T, Sugiyama A, Paris C, Hehn A, Bourgaud F, Yazaki K. 2014. A coumarin-specific prenyltransferase catalyzes the crucial biosynthetic reaction for furanocoumarin formation in parsley. The Plant Journal **77**, 627–638.

Kelly LJ, Plumb WJ, Carey DW, Mason ME, Cooper ED, Crowther W, Whittemore AT, Rossiter SJ, Koch JL, Buggs RJA. 2020. Convergent molecular evolution among ash species resistant to the emerald ash borer. Nature Ecology & Evolution doi: 10.1038/s41559-020-1209-3.

Kirisits T, Matlakova M, Mottinger-Kroupa S, Halmschlager E, Lakatos F. 2010. *Chalara fraxinea* associated with dieback of narrow-leafed ash (*Fraxinus angustifolia*). Plant Pathology **59**, 411.

Kostova I, Iossifova T. 2007. Chemical components of *Fraxinus* species. Fitoterapia **78**, 85–106.

Kowalski T. 2006. *Chalara fraxinea* sp. nov. associated with dieback of ash (*Fraxinus excelsior*) in Poland. Forest Pathology **36**, 264–270.

Lobo A, Hansen JK, McKinney LV, Nielsen LR, Kjær ED. 2014. Genetic variation in dieback resistance: growth and survival of *Fraxinus excelsior* under the influence of *Hymenoscyphus pseudoalbidus*. Scandinavian Journal of Forest Research **29**, 519–526.

McMullan M, Rafiqi M, Kaithakottil G, *et al*. 2018. The ash dieback invasion of Europe was founded by two genetically divergent individuals. Nature Ecology & Evolution **2**, 1000–1008.

Mercer DK, Robertson J, Wright K, Miller L, Smith S, Stewart CS, Deborah A. 2013. A prodrug approach to the use of coumarins as potential therapeutics for superficial mycoses. PLoS One **8**, e80760.

Muñoz F, Marçais B, Dufour J, Dowkiw A. 2016. Rising out of the ashes: additive genetic variation for crown and collar resistance to *Hymenoscyphus fraxineus* in *Fraxinus excelsior*. Phytopathology **106**, 1535–1543.

Nemesio-Gorriz M, McGuinness B, Grant J, Dowd L, Douglas GC. 2019. Lenticel infection in *Fraxinus excelsior* shoots in the context of ash dieback. iForest-Biogeosciences and Forestry **12**, 160.

Nemesio-Gorriz M, Menezes RC, Paetz C, Hammerbacher A, Steenackers M, Schamp K, Höfte M, Svatoš A, Gershenzon J, Douglas GC. 2020. Data from: Canditate metabolites for ash dieback tolerance in *Fraxinus excelsior*. Dryad Digital Repository. doi:10.5061/dryad.7m0cfxpqv

Niculaes C, Morreel K, Kim H, Lu F, McKee LS, Ivens B, Haustraete J, Vanholme B, De Rycke R, Hertzberg M. 2014. Phenylcoumaran benzylic ether reductase prevents accumulation of compounds formed under oxidative conditions in poplar xylem. The Plant Cell **26**, 3775–3791.

Ockels FS, Eyles A, McPherson BA, Wood DL, Bonello P. 2007. Phenolic chemistry of coast live oak response to *Phytophthora ramorum* infection. Journal of Chemical Ecology **33**, 1721–1732.

Petkovsek MM, Stampar F, Veberic R. 2007. Parameters of inner quality of the apple scab resistant and susceptible apple cultivars (*Malus domestica* Borkh.). Scientia Horticulturae **114**, 37–44.

Plumb WJ, Coker TL, Stocks JJ, Woodcock P, Quine CP, Nemesio-Gorriz M, Douglas GC, Kelly LJ, Buggs RJ. 2019. The viability of a breeding programme for ash in the British Isles in the face of ash dieback. Plants, People, Planet **2**, 29–40.

Qazi S, Lombardo D, Abou-Zaid M. 2018. A metabolomic and HPLC-MS/MS analysis of the foliar phenolics, flavonoids and coumarins of the *Fraxinus* species resistant and susceptible to emerald ash borer. Molecules **23**, 2734.

Sambles CM, Salmon DL, Florance H, Howard TP, Smirnoff N, Nielsen LR, McKinney LV, Kjær ED, Buggs RJA, Studholme DJ. 2017. Ash leaf metabolomes reveal differences between trees tolerant and susceptible to ash dieback disease. Scientific Data **4**, 170190.

Shimizu B. 2014. 2-Oxoglutarate-dependent dioxygenases in the biosynthesis of simple coumarins. Frontiers in Plant Science **5**, 549.

Smith CA, Want EJ, O'Maille G, Abagyan R, Siuzdak G. 2006. XCMS: processing mass spectrometry data for metabolite profiling using nonlinear peak alignment, matching, and identification. Analytical Chemistry **78**, 779–787.

Sollars ESA, Harper AL, Kelly LJ, Sambles CM, Ramirez-Gonzalez RH, Swarbreck D, Kaithakottil G, Cooper ED, Uauy C, Havlickova L. 2017. Genome sequence and genetic diversity of European ash trees. Nature **541**, 212.

Stener L-G. 2018. Genetic evaluation of damage caused by ash dieback with emphasis on selection stability over time. Forest Ecology and Management **409**, 584–592.

Stocks JJ, Metheringham CL, Plumb WJ, Lee SJ, Kelly LJ, Nichols RA, Buggs RJA. 2019. Genomic basis of European ash tree resistance to ash dieback fungus. Nature Ecology & Evolution **3**, 1686–1696.

Tautenhahn R, Böttcher C, Neumann S. 2008. Highly sensitive feature detection for high resolution LC/MS. BMC Bioinformatics **9**, 504.

Vanholme R, Sundin L, Seetso KC, Kim H, Liu X, Li J, De Meester B, Hoengenaert L, Goeminne G, Morreel K. 2019. COSY catalyses *trans–cis* isomerization and lactonization in the biosynthesis of coumarins. Nature Plants **5**, 1066–1075.

Villari C, Dowkiw A, Enderle R, *et al*. 2018. Advanced spectroscopy-based phenotyping offers a potential solution to the ash dieback epidemic. Scientific Reports **8**, 17448.

Villari C, Herms DA, Whitehill JG, Cipollini D, Bonello P. 2016. Progress and gaps in understanding mechanisms of ash tree resistance to emerald ash borer, a model for wood-boring insects that kill angiosperms. New Phytologist **209**, 63–79.

Wang M, Carver JJ, Phelan VV, *et al*. 2016. Sharing and community curation of mass spectrometry data with global natural products social molecular networking. Nature Biotechnology **34**, 828.

Wheat CW, Vogel H, Wittstock U, Braby MF, Underwood D, Mitchell-Olds T. 2007. The genetic basis of a plant–insect coevolutionary key innovation. Proceedings of the National Academy of Sciences, USA **104**, 20427–20431.

Whitehill JG, Opiyo SO, Koch JL, Herms DA, Cipollini DF, Bonello P. 2012. Interspecific comparison of constitutive ash phloem phenolic chemistry reveals compounds unique to manchurian ash, a species resistant to emerald ash borer. Journal of Chemical Ecology **38**, 499–511.

Whitehill JG, Popova-Butler A, Green-Church KB, Koch JL, Herms DA, Bonello P. 2011. Interspecific proteomic comparisons reveal ash phloem genes potentially involved in constitutive resistance to the emerald ash borer. PLoS One **6**, e24863.